Modification of water yam (*Dioscorea alata*) starch using thermal cyclic retrogradation: changes in structural, physicochemical properties and glycaemic index

KHANH SON TRINH – MINH HAI NGUYEN – TIEN GIANG NGUYEN – VINH TIEN NGUYEN

Summary

As a primary dietary carbohydrate, starch can be modified to influence its digestibility and glycaemic response. Such modifications are crucial for developing food products aimed at mitigating chronic metabolic diseases, including diabetes and obesity. For the first time, we modified gelatinized water yam (*Dioscorea alata*) starch using a cyclic thermal retrogradation approach (1–9 cycles of 4 °C for 18 h then 30 °C for 6 h). The modification significantly altered the starch's physicochemical, structural properties, and glycaemic index. Increasing retrogradation cycles correlated positively with syneresis, intrinsic viscosity, average molecular weight, degree of polymerization, and degree of relative crystallinity (*DRC*), while correlating negatively with amylose leaching, paste clarity, swelling power, and solubility. Fourier-transform infrared spectroscopy indicated progressive increases in molecular order and the emergence of new absorbance peaks. X-ray diffraction analysis confirmed a conserved B-type crystalline structure, but *DRC* increased with cycle number. Crucially, all retrograded starches displayed significantly reduced estimated glycaemic index (*eGI*) values relative to native starch; the sample after 9 thermal cycles yielded the lowest *eGI*. These findings demonstrate that cyclic thermal processing effectively modifies yam starch structure, enhancing crystallinity and substantially lowering its glycaemic response, making it a promising ingredient for developing functional foods beneficial for individuals with dietary restrictions or diabetes.

Keywords

water yam starch; retrogradation; starch modification; structural characteristics; physicochemical properties; glycaemic index

Dioscorea alata, or water yam, is a staple crop originating in Africa and Asia, now cultivated globally in tropical regions [1]. It is crucial for diet and economics in West Africa, the Caribbean, parts of Asia, and Oceania, second only to cassava and sweet potato. While over 600 *Dioscorea* species exist, six are widely cultivated, including *D. alata*, known for high yield and long storage. Other species have food and medicinal uses. *D. alata* typically contains 7.4 % crude protein, 75–84 % starch, and 130–247 mg·kg^{-1} vitamin C, with generally cylindrical tubers and flesh ranging from white to purple [2]. Tubers can reach 2–3 m and 50 kg. Water yam is a rich carbohydrate source, also providing potassium, and fibre (higher than potato, corn or rice), contributing slow glucose release. Anthocyanins and carotenoids provide tuber flesh pigmentation [3].

Starch retrogradation is the process where disassociated amylose and amylopectin chains in gelatinized starch are re-associated into crystalline regions. This process occurs in three stages: (1) nucleation – the formation of initial nuclei; (2) propagation – crystal growth around these nuclei; and (3) maturation – crystal perfection or slow continued growth of crystalline regions [4]. Retrogradation is accompanied by various physicochemical changes, including increased paste viscosity and turbidity, gel formation, syneresis (water separation), and elevated crystallinity with the emergence of B-type crystals [5]. Specifically, the short outer branches of amylopectin (with a degree

Khanh Son Trinh, Minh Hai Nguyen, Tien Giang Nguyen, Vinh Tien Nguyen, Faculty of Chemical and Food Technology, Ho Chi Minh City University of Technology and Education, 1 Vo Van Ngan, Thu Duc Ward, 700000 Ho Chi Minh City, Vietnam.

Correspondence author:
Vinh Tien Nguyen, e-mail: tiennv@hcmute.edu.vn

© 2025 National Agricultural and Food Centre (Slovakia)

of polymerization around 15) rearrange, leading to the formation of these B-type crystals [6]. Retrogradation results in a more ordered starch structure, which is less susceptible to enzymatic digestion, and consequently, leads to a slower release of glucose into the bloodstream [7]. This characteristic is highly desirable for developing functional food products aimed at managing postprandial glycaemic responses, particularly relevant for individuals with diabetes or those seeking healthier dietary options [8, 9].

While conventional starch retrogradation often occurs under static conditions, thermal cyclic retrogradation involves repeated cycles of cooling and warming. This dynamic process is designed to enhance the re-crystallization and structural ordering of starch by optimizing conditions for both nucleation (favoured at lower temperatures) and crystal growth (enhanced at higher temperatures) within each cycle. Unlike single-stage retrogradation, thermal cycling can lead to more stable and extensive crystalline structures, particularly the formation of B-type crystallites, due to the continuous rearrangement and annealing of starch molecules [10]. This unique approach offers a promising non-chemical method to modify starch, potentially improving its functional properties such as water binding capacity, paste clarity, and importantly, reducing its susceptibility to enzymatic digestion, thereby influencing its glycaemic response.

Despite the established understanding of starch retrogradation, the specific impact of cyclic thermal retrogradation on the comprehensive structural, physicochemical, and glycaemic properties of water yam starch remains underexplored. We hypothesize that repeated cycles of cooling and warming will induce significant re-association of starch chains, leading to enhanced crystallinity and molecular order, thereby altering its functional characteristics and reducing its glycaemic index. Therefore, the objective of this study was to systematically investigate the effect of varying cycles of thermal retrogradation on the structural characteristics, physicochemical properties, and in vitro glycaemic index of water yam starch, aiming to elucidate its potential as a low-glycaemic functional ingredient for food applications.

MATERIALS AND METHODS

Starch isolation

Water yam starch was isolated according to the method described in a previous research [10]. Water yam tubers purchased at a local market in Vietnam were thoroughly washed, peeled, and cut into smaller pieces. These pieces were then ground into slurry using a domestic blender with the addition of distilled water at 1 $ml \cdot g^{-1}$ to facilitate the grinding. The resulting slurry was filtered with muslin cloths to remove fibrous material and insoluble residues. Starch milk was subsequently collected and allowed to settle for 12 h. The settled starch cake was then repeatedly washed with distilled water to remove soluble impurities and pigments. Finally, the purified starch slurry was dried at 40 °C using forced convection, and then ground into a fine powder for storage.

Thermal cyclic starch retrogradation

Retrograded yam starch was produced using a cyclic thermal process. First, a water yam starch suspension (100 $g \cdot l^{-1}$) was pre-gelatinized in a water bath at 95 °C for 30 min. Then, the suspension underwent further gelatinization in an autoclave at 121 °C for 30 min before being cooled to room temperature (28 ± 1 °C). Next, the starch suspension was subjected to cyclic cooling (4 °C for 18 h) and warming (30 °C for 6 h), with each cycle lasting 24 h, repeated for 9 cycles [11]. After completing the cycles, the starch gel was spread into thin layers and dried using forced convection at 45 °C until its moisture content was reduced to below 10 %. The retrograded starch samples were collected as dry powders and coded as follows: R0 (gelatinized, but not retrograded) and R1, R3, R6, R9 were retrograded starches with 1, 3, 6, 9 thermal cycles, respectively. Besides that, the N sample (native starch, no treatment) was also used for comparison.

Structural characteristics of retrograded starches

Fourier-transform infrared spectroscopy

Fourier-transform infrared (FTIR) spectra of the starch powders were acquired using an FT/IR 4700 spectrometer (Jasco, Tokyo, Japan) equipped with an attenuated total reflectance (ATR) accessory. For each measurement, approximately 0.1 g of the dry starch sample was firmly compressed onto the ATR crystal. The spectrometer then recorded the infrared absorption intensity across the wavenumber range from 400 cm^{-1} to 4 000 cm^{-1} with a resolution of 2 cm^{-1} [12].

X-ray diffraction

X-ray diffraction (XRD) patterns of the starch samples were recorded using D8 Advance Eco equipment (Bruker, Bremen, Germany) at 40 kV and 40 mA with Cu – Kα radiation wavelength of 0.15406 nm, and a scanning angle (2θ) of 3–30°.

The degree of relative crystallinity (*DRC*) was calculated using the Eq. 1 [13] and expressed in percent:

$$DRC = \frac{A_a}{A_c + A_a} \times 100 \quad (1)$$

in which, A_c, A_a denote the area of the crystalline region and the area of the amorphous region, respectively. The reducing power of starches was determined according to published report [14].

Apparent amylose content

Apparent amylose content (*AAC*) of the starch samples was determined using the method of starch-iodine complex [15]. This involved accurately weighing 100.0 ± 0.1 mg of dry starch into a 100-ml volumetric flask, wetting it with 1 ml of ethanol, and dissolving it completely in 10 ml of 1 mol·l^{-1} NaOH solution for 1 h. After diluting to volume 100 ml with distilled water, a 2 ml aliquot was transferred to another 100-ml flask. This aliquot was neutralized with 0.1 mol·l^{-1} HCl using phenolphthalein indicator, followed by the addition of 2.0 ml of I_2–KI solution (0.2 g·l^{-1} I_2 and 2 g·l^{-1} KI). The final solution was then diluted to volume 100 ml and allowed to sit for 30 min for full colour development. Finally, the sample's absorbance was measured at 620 nm using a UH5300 UV-Vis spectrophotometer (Hitachi, Tokyo, Japan). A standard curve prepared with known concentrations of pure potato amylose (Sigma-Aldrich, St. Louis, Missouri, USA) was used to quantify the *AAC* of the starch samples.

Average molecular weight

The average molecular weight (M_W) of starch was calculated using intrinsic viscosity (η_i, expressed in litres per kilogram) of its solution, according to the Staudinger-Mark-Houwink equation (Eq. 2). Intrinsic viscosity was determined as the reduced viscosity η_{red} of the starch solution at extremely low starch concentration (Eq. 3), and was calculated using Eq. 4 [16].

$$\eta_i = K{M_W}^a \quad (2)$$

$$\eta_i = \lim_{c \to 0} \eta_{red} \quad (3)$$

in which, $K = 1.18 \times 10^{-3}$, $a = 0.89$, c is a concentration of starch gel. M_W is expressed in grams per mole) of starch [17].

$$\eta_{red} = \frac{\eta_{rel} - 1}{c} \quad (4)$$

with η_{rel} being the relative viscosity of the solution and calculated according to Eq. 5, in which, η represents the dynamic viscosity of the sample, η_0 is the dynamic viscosity of the blank 1 mol·l^{-1} KOH solution, t and t_0 (in seconds) are the flow times of the sample solution and the 1 mol·l^{-1} KOH through an Ostwald capillary viscometer (diameter of 0.3 mm, Fisher Scientific, Waltham, Massachusetts, USA), ρ is the density of the starch solution in 1 mol·l^{-1} KOH solution, and ρ_0 is the density of the blank 1 mol·l^{-1} KOH solution.

$$\eta_{rel} = \frac{\eta}{\eta_0} = \frac{t}{t_0} \times \frac{\rho}{\rho_0} \quad (5)$$

The dynamic viscosity η was calculated according to Eq. 6.

$$\eta = 0.004 \times t - \frac{0.12}{t} \quad (6)$$

Physicochemical characteristics of retrograded starches

Amylose leaching content

Amylose leaching content (*AML*) was determined according to method of Denchai et al. [7] with slight modifications to suit water yam starch samples.

A starch gel (0.5 g) obtained after cyclic thermal retrogradation was mashed into a uniform paste. This paste was then mixed with 20 ml of distilled water and centrifuged at 3 000 ×*g* for 10 min. After centrifugation, 2.0 ml of the supernatant (containing leached amylose) was carefully collected and transferred into a 20-ml volumetric flask containing 10 ml of distilled water. Subsequently, 2.0 ml of an I_2–KI solution (0.2 g·l^{-1} I_2 and 2 g·l^{-1} KI) was added, and the final volume of the solution was adjusted to 20 ml with distilled water. The tested solution was allowed to equilibrate for 20 min in the dark for full colour development and its absorbance at 620 nm was measured by a UH5300 UV-Vis spectrophotometer. The amount of leached amylose in the solution was calculated using the amylose standard curve as described in the section of *AAC* determination.

The total amylose content in the gel was quantified using the method of *AAC* determination. Finally, *AML* was calculated as the percentage of total amylose leached into the supernatant relative to the total amylose in the gel sample.

Syneresis

Syneresis (*S*) was measured according to the published method [18] with slight modifications to suit the samples. After each thermal cycle, starch gels were centrifuged (2 000 ×*g*, 10 min). Syneresis *S* was the amount of water expelled from the gel and expressed in percent:

$$S = \frac{m_1}{m_0} \times 100 \quad (7)$$

where m_0 is the initial gel weight and m_1 is the weight of expelled water.

Solubility and swelling power

Solubility (*SB*) and swelling power (*SP*) of the starch samples were determined using the method of Amini et al. [19].

Paste clarity

Paste clarity of starch was expressed as the percentage of transmittance (*T*). Starch suspensions were prepared at concentrations ranging from 10 g·l^{-1} to 50 g·l^{-1} and gelatinized (95 °C, 30 min) with continuous stirring. The starch gels were then cooled to room temperature (28 ± 1 °C) and the transmittance *T* was measured at 640 nm using a UH5300 UV-Vis spectrophotometer [20].

Hydrolysis rate and estimated glycaemic index

The hydrolysis rate (*HR*) and estimated glycaemic index (*eGI*) of starches were determined using a modified version of a published method [21]. An enzyme solution (10 U·ml^{-1}) was prepared by dispersing α-amylase (0.1 ml, Novozymes, Bagsvaerd, Denmark) in 100 ml of sodium phosphate buffer (pH 6.9, Fisher Scientific) containing 0.05 g of NaN_3 (as a microbial inhibitor) and was pre-incubated at 37 °C. Starch samples (0.5 g) were dispersed in 25 ml of the same buffer (pH 6.9) and equilibrated at 37 °C with stirring gently for 10 min. Hydrolysis was initiated by adding 5 ml of the enzyme solution, maintaining constant temperature and stirring. Aliquots (1 000 μl) were withdrawn at 0 (immediately after enzyme addition), 20, 60, 90, 120, 150, 180, 210, 240, 270, 300, 330, 360, 390, 420, 450, and 480 min. Enzyme activity was terminated by adding 1 ml of 3,5-dinitrosalicylic acid (DNS) reagent (Fisher Scientific), followed by heating in a boiling water bath for 5 min.

Glucose concentration in the supernatant was quantified spectrophotometrically at 530 nm using the DNS method and a glucose standard curve [22]. Hydrolysis curves were generated from this data and fitted to a first-order kinetic model (Eq. 8) proposed by Goñi et al. [23]:

$$C = C_\infty(1 - e^{-kt}) \quad (8)$$

where C is the reducing sugar concentration at time t, C_∞ is the maximum concentration at infinite time, and k is the rate constant.

A control hydrolysis curve was generated using native starch, which was pre-gelatinized by boiling for 15 min and autoclaving at 121 °C for 10 min (sample R0). The *eGI* was estimated by calculating the area under the hydrolysis curve (*AUC*) in 0–180 min period for each sample using Origin 8.5.1 software (OriginLab, Northampton, Massachusetts, USA). The *eGI* was then expressed as the percentage of the *AUC* of the sample relative to the *AUC* of the gelatinized native water yam starch (defined as 100 %) [23].

Statistical analysis

All experiments were conducted in triplicate, and the mean results along with the standard deviations are provided in the results section after statistical analysis. ANOVA was used to analyse variance, and the differences between mean values were assessed using Duncan's test ($p < 0.05$) with SPSS software version 22 (SPSS, Chicago, Illinois, USA).

RESULTS AND DISCUSSION

Structural characteristics of starch samples

Fourier-transform infrared spectroscopy analysis

FTIR analysis is a rapid, non-destructive, and precise technique used in the food industry to analyse molecular interactions and structural transitions in carbohydrates. It has also been used to quickly check the status of starch before, during, and after retrogradation. The ratio of absorbance bands at 1 047 cm^{-1}/1 022 cm^{-1} can indicate the degree of starch crystallinity. FTIR analysis results of starch samples are shown in the Fig. 1. While the overall spectral shapes were similar, the absorption intensities varied considerably, indicating changes in the chemical bond tightness between samples.

Key spectral regions include < 800 cm^{-1} (pyranose ring vibrations), 800–1 500 cm^{-1} (glucose vibrations), and 3 000–3 600 cm^{-1} (O-H stretching). A 930 cm^{-1} band indicates glycosidic linkages [24]. Retrogradation-induced structural changes were observed via band intensities in the 800–1 300 cm^{-1} region. Specifically, band narrowing between 950–1 050 cm^{-1}, with a 1 019 cm^{-1} band emerging (prominent in R9) from a broad 1 022 cm^{-1} band in R0, signified double-helix formation. This contrasted with the single broad 1 022 cm^{-1} band (R0).

Furthermore, the width and height of the bands at 3 000–3 800 cm^{-1} and 1 637 cm^{-1} differed significantly among samples, decreasing in the order N > R0 > R1 > R3 > R6 > R9. This observed reduction in the intensity and broadening of the O-H stretching region (3 000–3 800 cm^{-1}) signifies a decrease in free and weakly-bound water, imply-

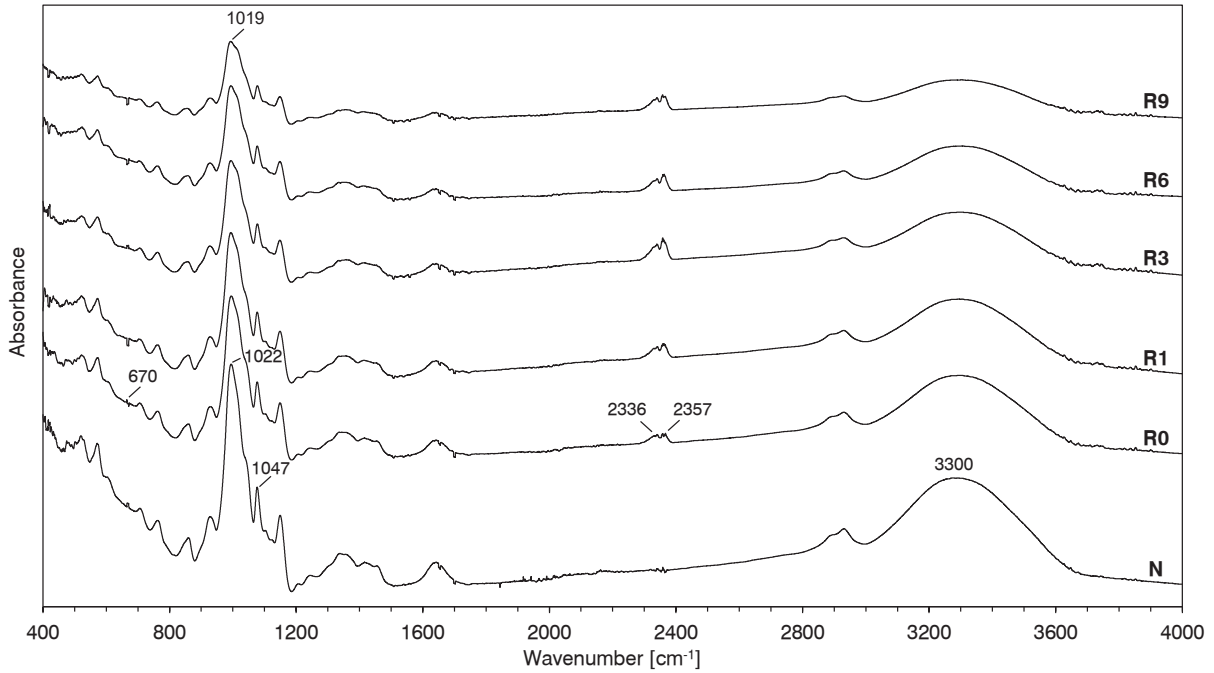


Fig. 1. Fourier-transform infrared spectroscopy spectrum of starch samples.

N – native starch; R0 – gelatinized, not retrograded starch; R1, R3, R6, R9 – starches subjected 1, 3, 6, 9 thermal cycles of retrogradation, respectively.

ing alterations in hydrogen bonding networks and a more ordered, less hydrated starch structure. Similarly, the diminished 1 637 cm^{-1} band, characteristic of water tightly bound to amorphous regions, further supports a reduction in water interactions within the starch matrix, leading to increased crystallinity. These changes collectively suggest significant conformational changes in starch chains, facilitating their re-association and the formation of more stable crystalline structures upon retrogradation, particularly the B-type polymorph [12].

Compared to N sample, three new peaks at 670 cm^{-1}, 2336 cm^{-1}, and 2357 cm^{-1} appeared in R samples. The appearance of the new peak at 670 cm^{-1} is often associated with the C-O-C bending vibrations within the polysaccharide structure and can suggest changes in the helical conformation or even limited chain degradation induced by the thermal processing [25]. Furthermore, the emergence of peaks at 2 336 cm^{-1} and 2 357 cm^{-1} in the retrograded samples, which were absent in native starch, are typically attributed to the stretching vibrations of C=O bonds. While these peaks are sometimes related to the presence of CO_2 in the air, their consistent appearance and increasing intensity with retrogradation cycles could also indicate the formation of minor oxidative products or specific carbonyl functionalities due to the combined effects of heat and moisture during the extensive thermal cycling. Further investigation may be needed to fully elucidate their precise origins and implications. The ratio of absorbances at 1 047 cm^{-1} (α-helix) and 1 022 cm^{-1} (amorphous region) increased with retrogradation (Tab. 1), indicating a decrease in the amorphous regions and increase crystalline regions, supporting double helix formation [26]. This observed increase in crystallinity is a desired functional improvement for water yam starch. Enhanced crystallinity contributes to several beneficial properties, including a reduced susceptibility to enzymatic digestion, leading to a lower estimated glycaemic index, which is highly advantageous for developing functional foods. Furthermore, increased crystallinity can positively influence textural attributes such as gel firmness and reduced stickiness, and improve physical stability by minimizing syneresis, thereby enhancing the overall quality and application potential of the modified starch in various food formulations.

The results showed that the retrogradation process caused changes in the α-helix/amorphous region ratio of the retrograded starch samples. In our experiment, sample R9 had a higher α-helix/amorphous region ratio than the native yam starch sample.

Tab. 1. Relationship between infrared absorption ratios and starch crystallinity.

Samples	Absorbance		A_2/A_1	*DRC* [%]
	A_1 (1 022 cm^{-1})	A_2 (1 047 cm^{-1})		
N	0.4945	0.3823	0.7730 ^{e}	67.6 ± 0.1 ^{d}
R0	0.4554	0.3322	0.7294 ^{a}	20.4 ± 0.1 ^{a}
R1	0.4462	0.3264	0.7315 ^{b}	42.6 ± 0.1 ^{b}
R3	0.4761	0.3520	0.7394 ^{c}	56.7 ± 0.1 ^{c}
R6	0.5229	0.3961	0.7575 ^{d}	68.2 ± 0.1 ^{e}
R9	0.5002	0.3878	0.7753 ^{f}	73.2 ± 0.1 ^{f}

Values with different letters in the same column indicate statistically significant differences ($p < 0.05$).
N – native starch; R0 – gelatinized, not retrograded starch; R1, R3, R6, R9 – starches subjected 1, 3, 6, 9 thermal cycles of retrogradation, respectively.
A_1, A_2 – absorbances measured by FTIR spectroscopy; A_2/A_1 – α-helix/amorphous ratio; *DRC* – degree of relative crystallinity deduced from X-ray diffraction spectra.

X-ray diffraction analysis

XRD patterns of native (N) and retrograded (R1, R3, R6, R9) water yam starch samples are presented in Fig. 2, with corresponding *DRC* values listed in Tab. 1. The native starch (N) exhibited a characteristic B-type crystalline structure, displaying major peaks at approximately 5.7° and 17.1° (2θ) and minor peaks at 15.1°, 22.4°, and 24.1° (2θ) [5]. This B-type polymorph was consistent with previous findings for native water yam starch [10]. The fully gelatinized starch (R0) showed a completely amorphous XRD pattern, devoid of any diffraction peaks, confirming the loss of crystalline order due to gelatinization. The retrograded samples (R1, R3, R6 and R9) all maintained the B-type crystalline pattern, indicating no change in the crystalline polymorph. However, there was a clear trend of increasing peak intensity with increasing thermal cycle number (R1 < R3 < R6 < R9). Samples R6 and R9 exhibited all characteristic B-type peaks, while R1 and R3 showed a prominent peak mainly around 5.7° (2θ), indicative of initial B-type crystallite formation [10].

Fig. 2 illustrates that with an increasing number of thermal cycles, there is an enhancement in the intensity of the diffraction peaks. While an increase in diffraction intensity does not always

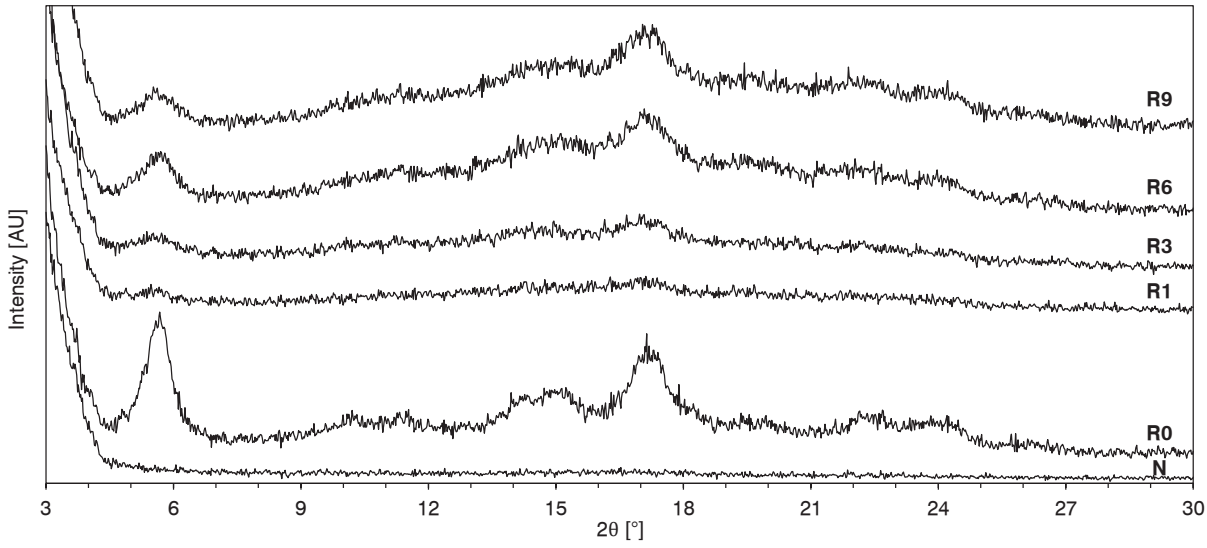


Fig. 2. X-ray diffraction patterns of starch samples.

N – native starch; R0 – gelatinized, not retrograded starch; R1, R3, R6, R9 – starches subjected 1, 3, 6, 9 thermal cycles of retrogradation, respectively.

directly equate to a rise in overall crystallinity [27], the *DRC* values (Tab. 1) indeed demonstrate a progressive increase in the relative crystallinity of the starch samples with a greater number of thermal processing cycles. R0 had the lowest *DRC* (20.4 %), confirming its amorphous nature. The retrograded samples showed a progressive increase in *DRC*: R1 (42.6 %) < R3 (56.7 %) < R6 (68.2 %) < R9 (73.2 %). The observed increase in overall starch crystallinity with a higher number of thermal cycling treatments is primarily due to the enhanced and optimized retrogradation process. Each cycle of cooling and warming facilitates the formation of initial crystalline nuclei during cooling and promotes their growth and stabilization during warming. This repeated, dynamic re-association allows for the formation of more extensive and stable hydrogen bonding networks within the starch chains, leading to a higher proportion of well-ordered crystalline regions, particularly the B-type polymorph.

Notably, R6 and R9 exhibited *DRC* values higher than the native starch (67.6 %). This suggested a greater degree of crystalline order in these retrograded samples, a result that contrasted with some studies on potato starch where retrograded samples had lower *DRC* than the native material. This enhanced retrogradation in water yam starch might be attributed to its higher amylose content, which promoted crystallization. The thermal cycling (4 °C/18 h – 30 °C/6 h) likely optimized the balance between nucleation (favoured at lower temperatures) and propagation (enhanced at higher temperatures), contributing to the increased *DRC* [28]. This finding of

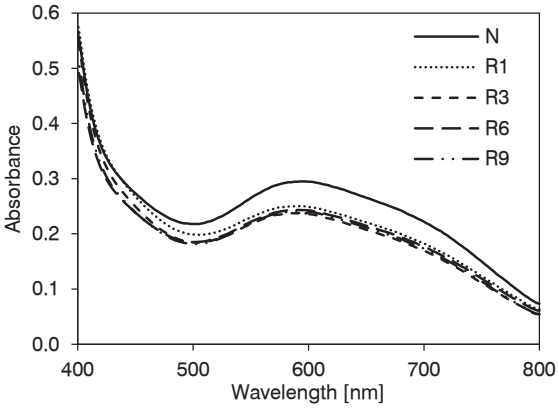


Fig. 3. Starch-iodine complex absorption spectrum of starch samples.

N – native starch; R0 – gelatinized, not retrograded starch; R1, R3, R6, R9 – starches subjected 1, 3, 6, 9 thermal cycles of retrogradation, respectively.

significantly increased crystallinity, as quantified by *DRC*, strongly corroborates and reinforces the observations from the FTIR analysis, where the increasing α-helix/amorphous ratio also indicated enhanced molecular order and crystalline region formation in the retrograded samples. The functional benefits associated with such increased crystallinity, including reduced enzymatic digestibility and improved textural properties, have been discussed in detail in the FTIR section.

Differences between FTIR (α-helix/amorphous ratio) and XRD (*DRC*) results were observed, for instance, native starch (N) showed an A_2/A_1 ratio of 0.7730 (77.3 %) via FTIR, while its *DRC* from XRD was 67.6 %. While both techniques provide valuable insights into the ordered structures within starch, the numerical discrepancies in their crystallinity assessments are primarily attributable to the fundamental differences in their measurement principles and sensitivities. FTIR assesses the degree of molecular order based on characteristic vibrational modes of starch functional groups, whereas XRD quantifies crystallinity based on the long-range periodic arrangement of molecules within crystalline domains.

Apparent amylose content

The functional properties of starch are significantly influenced by the amylose/amylopectin ratio, affecting gelatinization, solubility, viscosity, texture, and resistant starch formation [6]. *AAC* and iodine-starch complex absorption spectra provide insights into these structural changes. Fig. 3 shows two primary trends: (1) All retrograded starch samples (R1–R9) exhibited lower peak absorbance and *AAC* compared to native starch (N). (2) Retrograded samples showed a slight increase in peak absorbance and *AAC* in the order R1 < R3 < R6 < R9. The lower peak absorbance and *AAC* in retrograded starches (trend 1) related to a decreased chain length. A linear relationship exists between glucan chain length and its iodine-binding affinity; shorter chains bind less iodine, leading to lower absorbance wavelengths [29]. This aligns with previous results showing depolymerisation during gelatinization, increasing reducing ends, reducing average molecular weight and degree of polymerization. While such depolymerisation results in shorter starch chains, these shorter chains possess higher mobility and less entanglement, which can facilitate their re-association and enhance the rate and extent of crystallization during subsequent retrogradation. Therefore, in the context of producing a low-glycaemic starch, this initial reduction in chain length followed by re-association can con-

Tab. 2. The chemical structural characteristics of the starch samples.

Samples	η_i [l·kg^{-1}]	M_W [$\times 10^5$ g·mol^{-1}]	*AAC* [%]	*AML* [%]	*RP* [g·kg^{-1}]
N	233.60 ± 0.00 ^{d}	8.94 ± 0.00 ^{d}	17.3 ± 0.1 ^{e}	17.3 ± 0.1 ^{d}	3.79 ± 0.07 ^{c}
R0	143.45 ± 7.09 ^{a}	5.17 ± 2.87 ^{a}	NA	NA	15.38 ± 0.07 ^{f}
R1	211.07 ± 3.55 ^{b}	7.97 ± 1.51 ^{b}	12.3 ± 0.4 ^{a}	5.5 ± 0.1 ^{c}	4.50 ± 0.02 ^{e}
R3	215.16 ± 0.00 ^{bc}	8.15 ± 0.00 ^{bc}	13.3 ± 0.1 ^{b}	0.7 ± 0.1 ^{b}	4.26 ± 0.08 ^{d}
R6	217.21 ± 3.55 ^{bc}	8.24 ± 1.51 ^{bc}	13.4 ± 0.1 ^{c}	0.1 ± 0.1 ^{a}	3.26 ± 0.01 ^{b}
R9	221.31 ± 0.00 ^{c}	8.41 ± 0.00 ^{c}	13.7 ± 0.2 ^{d}	0.0 ± 0.0 ^{a}	3.12 ± 0.02 ^{a}

Values with different letters in the same column indicate statistically significant differences ($p < 0.05$).
N – native starch; R0 – gelatinized, not retrograded starch; R1, R3, R6, R9 – starches subjected 1, 3, 6, 9 thermal cycles of retrogradation, respectively.
η_i – intrinsic viscosity; M_W – average molecular weight; *AAC* – apparent amylose content; *AML* – amylose leaching content; *RP* – reducing power; NA – not applicable.

tribute positively to the desired functional outcome by promoting the formation of resistant crystalline structures.

The slight increase in AAC and peak absorbance from R1 to R9 (trend ii) correlated with decreasing reducing power, and increasing molecular weight (Tab. 2). This was the result of molecule re-association. However this re-association did not create a perfect chain, resulting in an overall chain lengthening, and slight impact on amylose-iodine formation [30].

Average molecular weight

M_W is a critical parameter influencing the functional and processing characteristics of polymers, including starch [31]. While techniques such as gel permeation chromatography (GPC) offer absolute M_W determination, solution viscometry provides a simple, cost-effective, and valuable method for assessing changes in polymer size and conformation, particularly for comparative studies.

In this study, we investigated the molecular characteristics of water yam starch through reduced viscosity (η_{red}) and intrinsic viscosity (η_i). Reduced viscosity reflects the increase in viscosity of a polymer solution due to the presence of the solute, normalized by concentration, and is therefore concentration-dependent. In contrast, intrinsic viscosity represents the inherent hydrodynamic volume of isolated polymer macromolecules in solution, extrapolated to infinite dilution, and is independent of concentration. It provides crucial insights into the polymer's size, shape, and interactions with the solvent. The average M_W was then estimated using the Staudinger-Mark-Houwink equation (Eq. 3), which relates intrinsic viscosity to molecular weight for a given polymer-solvent system. While this method yields a relative, not absolute, indication of M_W, it is highly effective for monitoring changes in average chain length and molecular association during processing.

The η_{red} of water yam starch solutions increased linearly with concentration, following the order: R0 < R1 < R3 < R6 < R9 < N at each concentration (Fig. 4). This linear relationship indicates increasing starch-solvent (KOH) interactions and frictional forces as starch dispersion increases in solution. [16]. The dramatic decrease in both η_i and M_W from native starch (N) to gelatinized starch (R0) (Tab. 2) provides strong evidence for starch chain depolymerisation during the extensive gelatinization process, alongside the formation of amorphous regions. This depolymerisation is further supported by the concurrent increase in reducing ends in R0 (Tab. 2), as broken starch chains create new reducing termini.

Subsequently, the observed increase in η_i and M_W across the retrograded samples (R1, R3, R6,

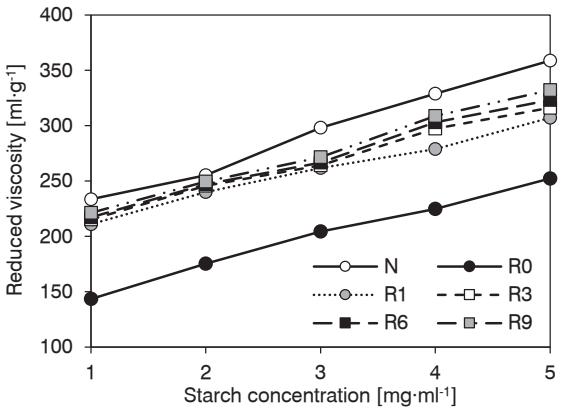


Fig. 4. Reduced viscosity of starch samples.

N – native starch; R0 – gelatinized, not retrograded starch; R1, R3, R6, R9 – starches subjected 1, 3, 6, 9 thermal cycles of retrogradation, respectively.

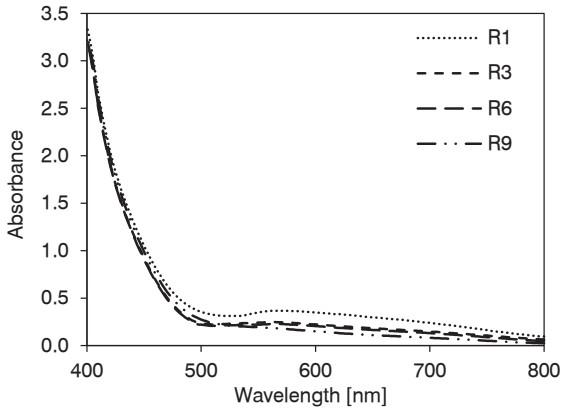


Fig. 5. Absorption spectrum of leached amylose-iodine complex.

R1, R3, R6, R9 – starches subjected 1, 3, 6, 9 thermal cycles of retrogradation, respectively.

and R9) signifies the occurrence of intermolecular hydrogen bonding and re-association of starch chains. During retrogradation, starch chains, including those depolymerized during gelatinization, begin to re-align and form more ordered structures. This re-association leads to larger effective hydrodynamic volumes, resulting in higher apparent M_W values [32]. The formation of stable double helices and B-type crystallites during retrogradation further contributes to higher viscosity by enhancing water absorption within the newly formed ordered structures and by hindering the diffusion and ionization of KOH within the more compact starch matrix [5].

Despite this re-association, the M_W of retrograded samples (R1, R3, R6 and R9) remained lower than that of native starch (N). This is attributed to the irreversible partial depolymerisation that occurred during the initial high-temperature gelatinization. The overall retrogradation process in water yam starch can therefore be understood as a two-stage phenomenon: initial complete gelatinization causes starch chain depolymerisation, leading to decreased average M_W and increased reducing ends in R0. Subsequently, in the retrogradation stage (R1, R3, R6, R9), depolymerized and/or intact starch chains reassociate. This reassociation results in a decrease in reducing ends and an increase in average M_W compared to R0. However, the M_W of retrograded samples, while increasing with cycles, did not fully recover to the level of native starch due to the preceding depolymerisation. The increase in these values across retrograded samples was progressive, with a statistically significant difference observed between R1 and R9.

Physicochemical characteristics of retrograded starches

Amylose leaching content

The leached amylose molecules have the mobility necessary to align and form double helices, which then aggregate to form crystalline structures. This is the fundamental basis of amylose retrogradation. *AML* decreased significantly from 17.3 % in native starch to 5.5 % after the first cycle (Fig. 5 and Tab. 2), indicating substantial retrogradation within the initial 24 h. During starch gelatinization, amylose leached from starch granules. Subsequent low-temperature storage promoted amylose-amylose intermolecular associations, reducing free amylose and, consequently, *AML*. The results aligned with results of previous reports, that observed high amylose leaching initially during retrogradation [33].

The significant reduction in *AML* is a crucial indicator of successful starch retrogradation, directly reflecting the re-association and re-crystallization of amylose chains into more ordered and resistant structures. This increased molecular order contributes directly to the reduced starch digestibility. Additionally, it improves textural properties and enhances the overall physical stability of the starch gel by limiting enzyme access and reducing water mobility, thereby decreasing syneresis.

Syneresis

Syneresis (Fig. 6), in conjunction with *AML*, reflects retrogradation trends [18]. From cycles 2 to 6, increasing syneresis and sharp *AML* decline indicated rapid amylose/amylose and amylose/amylopectin retrogradation. From cycles 7 to 9, minimal changes in syneresis and very low *AML* suggested retrogradation involving amylopec-

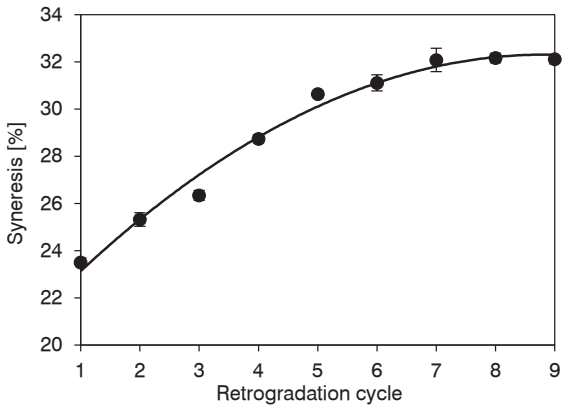


Fig. 6. Syneresis of starch gels with different retrogradation cycles.

tin outer branches, and stabilization of amylose/amylose and amylose/amylopectin double helices. A rapid increase in water separation was observed from cycle 1 (23.5 %) to cycle 5 (30.6 %). Subsequently, the rate of syneresis slowed, with no significant difference observed between cycle 7 (32.1 %) and cycle 9 (32.1 %). This increase in water separation was indicative of starch retrogradation, where the disrupted semi-crystalline structure of the starch granules (in gelatinization) reformed upon cooling. The amylose and amylopectin polymer chains re-associate, forming double helices through hydrogen bonding. This recrystallization process expelled water previously bound within the gel network, leading to increased syneresis [20]. Therefore, a higher degree of water separation correlates with increased starch retrogradation.

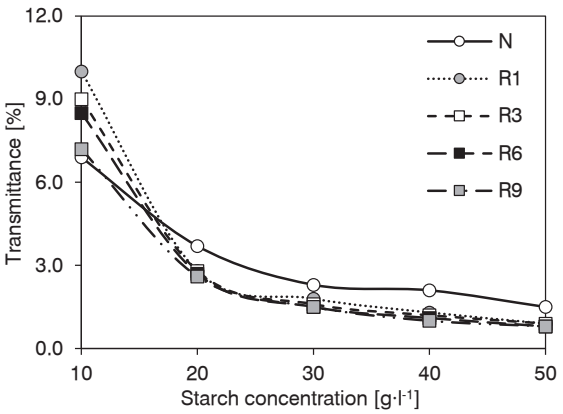


Fig. 7. Transmittance of starch pastes at different starch concentrations.

N – native starch; R1, R3, R6, R9 – starches subjected 1, 3, 6, 9 thermal cycles of retrogradation, respectively.

Transmittance

Starch paste transmittance (*T*) indicating clarity, reflects starch-water interactions and is influenced by granule size, swelling power, amylose leaching, amylose/amylopectin ratio, retrogradation, and the ratio of swollen to unswollen granules [29]. Fig. 7 shows that at 10 $g \cdot l^{-1}$ concentration, the paste of native starch (which is also sample R0) exhibited higher transmittance than all retrograded starch pastes, with increasing thermal treatment cycles further reducing the transmittance of the starch paste, following the order: N > R1 > R3 > R6 > R9. This result can be explained as follows: as the number of thermal treatment cycles increased, the degree of crystallinity rose, making the starch more resistant to complete gelatinization within 30 min at 95 °C. This resulted in a greater number of ungelatinized crystals, thereby increasing the turbidity of the starch paste. [33]. Fig. 7 shows that *T* decreases with increasing starch concentration. From a starch concentration of 20 $g \cdot l^{-1}$ upwards, the transmittance of the starch paste for all samples was very low (below 3 %) and showed no significant difference. This is because the large amount of starch did not undergo complete gelatinization, resulting in a high quantity of solid swollen starch that absorbed and scattered almost all light [34]. At such low transmittance, the spectrophotometer would have a large relative error and would not be able to distinguish between transmittance values.

Solubility and swelling

Starch solubility and swelling power, indicative of interactions between crystalline and amorphous regions, reflect amylose leaching and amylopectin characteristics, respectively [35]. Both parameters increased with temperature for all starch samples. Fig. 8 shows that below 65 °C, native starch (N) exhibited lower solubility and swelling than retrograded starches (R1 > R3 > R6 > R9), attributed to the native starch's robust semi-crystalline structure and strong intermolecular forces [33]. Retrograded starches, despite re-association and double helix formation, likely possessed more amorphous regions and incompletely/weakly retrograded molecules, facilitating greater hydration [4].

Above 65 °C, solubility and swelling of sample N sharply increased due to gelatinization and disruption of intramolecular bonds, allowing water penetration [7]. Retrograded starches, however, exhibited reduced swelling due to the more stable crystalline regions formed during retrogradation, hindering water diffusion [32], and also a decrease in solubility, due to the amylose reassociation. The increase in solubility and swelling power was observed from 45 °C onwards in the retrograded starches.

Among retrograded samples, increased retrogradation time (R1 to R9) resulted in decreased solubility and swelling, caused by stronger intermolecular bonding, impeding water diffusion. Similar trends have been reported. Increased temperature facilitated the disruption of intramolecular starch bonds, leading to crystalline structure breakdown and increased water penetration, thus increasing solubility and swelling power [36]. The low solubility and swelling power, coupled with the stability of these characteristics above 65 °C, make retrograded *Dioscorea alata* starch a promising ingredient for food applications requiring firmness and crispness, such as ready-to-eat cereals, biscuits, crackers, and bread.

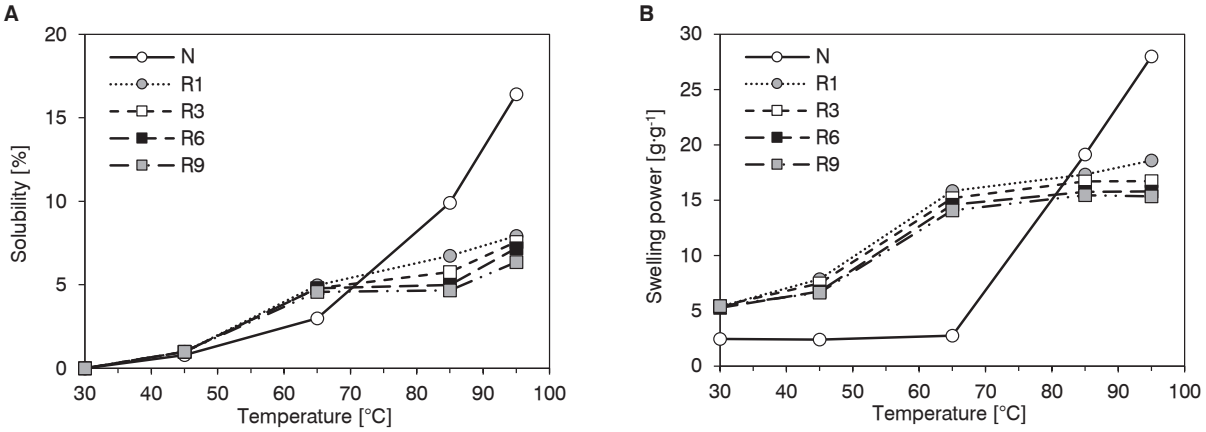


Fig. 8. Solubility and swelling power of starch samples at different temperatures.

A – solubility, B – swelling power.
N – native starch; R1, R3, R6, R9 – starches subjected 1, 3, 6, 9 thermal cycles of retrogradation, respectively.

Hydrolysis rate and estimated glycaemic index of retrogradation starch

In vitro digestion of gelatinized native (R0) and retrograded (R1, R3, R6 and R9) water yam starches was performed using α-amylase (10 U·ml^{-1}). Hydrolysis curves (Fig. 9) and kinetic parameters (Tab. 3) revealed that R0 exhibited the highest hydrolysis extent and rate. Retrograded starches (R1, R3, R6 and R9) showed significantly reduced hydrolysis rate (*HR*), with the extent of hydrolysis decreasing in the order: R0 > R1 > R3 > R6 > R9. The estimated glycaemic index (*eGI*) values (Tab. 3) correlated positively with hydrolysis extent. R0 exhibited an *eGI* of 100.0 ± 0.0 %, while retrograded samples showed a decreasing trend: R1 (63.1 %) > R3 (51.8 %) > R6 (50.5 %) > R9 (48.6 %). Therefore, R1 is classified as a medium *eGI* starch, while R3, R6, and R9 samples all fall within the low *eGI* category (< 55 %) [8].

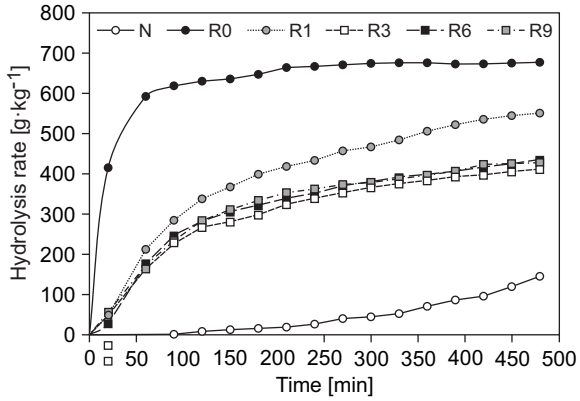


Fig. 9. Hydrolysis rate of different starch samples under the action of α-amylase.

Hydrolysis rate is expressed as grams of glucose per kilogram of starch.
N – native starch; R0 – gelatinized, not retrograded starch; R1, R3, R6, R9 – starches subjected 1, 3, 6, 9 thermal cycles of retrogradation, respectively.

The reduced hydrolysis and *eGI* of retrograded starches were attributed to microstructural modifications, specifically the formation of crystalline regions [7]. Increased crystalline structure in these samples was evidenced by decreased solubility and swelling power, and increased intrinsic viscosity, indicative of intermolecular hydrogen bonding and double helix formation [35]. Higher α-helix/amorphous ratios and increased *DRC* further confirmed enhanced crystal formation. These crystalline regions, formed from double helices, limit the starch surface area available for enzymatic attack, impeding enzyme diffusion and adsorption, thereby slowing glucose release [29]. The decreasing *eGI* trend (R1 > R3 > R6 > R9) directly reflected the impact of retrogradation time. Shorter retrogradation (R1) resulted in less perfect crystalline regions, allowing moderate enzyme diffusion and a medium *eGI* [37]. Longer retrogradation periods (R3, R6, R9) promoted more extensive hydrogen bonding and greater crystalline stability, further restricting enzyme accessibility [7]. Conversely, R0 (gelatinized starch) exhibited lower α-helix/amorphous ratios, lower *DRC*, and evidence of thermal degradation, reflecting a more porous crystalline structure. Gelatinization released starch chains, promoting subsequent rearrangement and stronger crystal formation during retrogradation [20]. Thermal degradation of starch chains during autoclaving may also positively correlate

Tab. 3. The estimated glycaemic index of starch samples.

Samples	C_∞ [g·kg^{-1}]	k [min^{-1}]	*eGI* [%]
R0	662.07	0.045 ^{a}	100.0 ± 0.0 ^{e}
R1	548.28	0.007 ^{b}	63.1 ± 0.1 ^{d}
R3	428.24	0.008 ^{c}	51.8 ± 0.2 ^{c}
R6	423.32	0.008 ^{c}	50.5 ± 0.5 ^{b}
R9	412.36	0.008 ^{c}	48.6 ± 0.1 ^{a}

Values with different letters in superscript in the same column indicate statistically significant differences ($p < 0.05$).
N – native starch; R0 – gelatinized, not retrograded starch; R1, R3, R6, R9 – starches subjected 1, 3, 6, 9 thermal cycles of retrogradation, respectively.
C_∞ – concentration of reducing sugar (represented by glucose) at infinite hydrolysis time; k – the hydrolysis rate constant from equation Eq. 8; *eGI* – estimated glycaemic index.

with stable crystal formation during retrogradation. Comparative studies demonstrated that yam starch tends to retrograde more effectively, resulting in greater crystallinity and lower *eGI*s, compared to rice and potato starches [7].

CONCLUSIONS

Thermal cycling treatment of water yam starch induced significant changes in physicochemical properties, including increased apparent amylose content, decreased paste clarity and swelling power, and increased intrinsic viscosity. XRD and FTIR analyses revealed that the thermal cycling did not alter the functional groups or crystalline type of the native starch. However, the *DRC* and the α-helix/amorphous ratio increased in the retrograded samples (R6 and R9), confirming enhanced crystalline region formation. In vitro enzymatic hydrolysis with α-amylase revealed that three out of four retrograded starch samples exhibited low *eGI* values. Sample R9 exhibited the lowest *eGI* (48.6 %). These results suggest that thermally cycled, retrograded water yam starch, with its enhanced crystallinity and reduced glycaemic response, has potential applications in food formulations, particularly for creating firm and crisp products like ready-to-eat cereals, crackers, and certain baked goods beneficial for individuals with dietary restrictions or diabetes.

Acknowledgements

This work was funded by the Ministry of Education and Training of Vietnam, under grant No. B2024-SPK-03, and hosted by Ho Chi Minh City University of Technology and Education, Vietnam. We sincerely acknowledge the technical assistance of Ms. Kim-Mai Nguyen (undergraduate student ID 18116089) who has supported us with enthusiasm and responsibility thereby helping to keep the research on schedule. We are also grateful to Ho Chi Minh University of Technology and Education for providing the facilities for us to carry out this study.

REFERENCES

1. Baah, F. D. – Maziya-Dixon, B. – Asiedu, R. – Oduro, I. – Ellis, W. O.: Nutritional and biochemical composition of *D. alata* (*Dioscorea* spp.) tubers. Journal of Food, Agriculture and Environment, *7*, 2009, pp. 373–378. ISSN: 1459-0255 (print), 1459-0263 (online).
2. Oko, A. O. – Famurewa, A. C.: Estimation of nutritional and starch characteristics of *Dioscorea alata* (water yam) varieties commonly cultivated in the South-Eastern Nigeria. Current Journal of Applied Science and Technology, *6*, 2015, pp. 145–152. DOI: 10.9734/BJAST/2015/14095.
3. Coursey, D. G.: Yams. An account of the nature, origins, cultivation and utilisation of the useful members of the Dioscoreaceae. London : Longmans, 1967.
4. Ambigaipalan, P. – Hoover, R. – Donner, E. – Liu, Q.: Retrogradation characteristics of pulse starches. Food Research International, *54*, 2013, pp. 203–212. DOI: 10.1016/j.foodres.2013.06.012.
5. Hoover, R.: Composition, molecular structure, and physicochemical properties of tuber and root starches: a review. Carbohydrate Polymers, *45*, 2001, pp. 253–267. DOI: 10.1016/S0144-8617(00)00260-5.
6. Hoover, R. – Hughes, T. – Chung, H. J. – Liu, Q.: Composition, molecular structure, properties, and modification of pulse starches: A review. Food Research International, *43*, 2010, pp. 399–413. DOI: 10.1016/j.foodres.2009.09.001.
7. Denchai, N. – Suwannaporn, P. – Lin, J. – Soontaranon, S. – Kiatponglarp, W. – Huang, T. C.: Retrogradation and digestibility of rice starch gels: the joint effect of degree of gelatinization and storage. Journal of Food Science, *84*, 2019, pp. 1400–1410. DOI: 10.1111/1750-3841.14633.
8. Venn, B. J. – Green, T. J.: Glycemic index and glycemic load: measurement issues and their effect on diet–disease relationships. European Journal of

Clinical Nutrition, *61*, 2007, pp. S122–S131. DOI: 10.1038/sj.ejcn.1602942.
9. Toh, D. W. K. – Koh, E. S. – Kim, J. E.: Lowering breakfast glycemic index and glycemic load attenuates postprandial glycemic response: A systematically searched meta-analysis of randomized controlled trials. Nutrition, *71*, 2020, article 110634. DOI: 10.1016/j.nut.2019.110634.
10. Trinh, K. S. – Choi, S. J. – Moon, T. W.: Structure and digestibility of debranched and hydrothermally treated water yam starch. Starch, *65*, 2013, pp. 679–685. DOI: 10.1002/star.201200149.
11. Muir, J. G. – O'Dea, K.: Measurement of resistant starch: factors affecting the amount of starch escaping digestion in vitro. The American Journal of Clinical Nutrition, *56*, 1992, pp. 123–127. DOI: 10.1093/ajcn/56.1.123.
12. Kizil, R. – Irudayaraj, J. – Seetharaman, K.: Characterization of irradiated starches by using FT-Raman and FTIR spectroscopy. Journal of Agricultural and Food Chemistry, *50*, 2002, pp. 3912–3918. DOI: 10.1021/jf011652p.
13. Nara, S. – Komiya, T.: Studies on the relationship between water-satured state and crystallinity by the diffraction method for moistened potato starch. Starch, *35*, 1983, pp. 407–410. DOI: 10.1002/star.19830351202.
14. Zhang, Z. – Zhao, S. – Xiong, S.: Morphology and physicochemical properties of mechanically activated rice starch. Carbohydrate Polymers, *79*, 2010, pp. 341–348. DOI: 10.1016/j.carbpol.2009.08.016.
15. Zhu, T. – Jackson, D. S. – Wehling, R. L. – Geera, B.: Comparison of amylose determination methods and the development of a dual wavelength iodine binding technique. Cereal Chemistry, *85*, 2008, pp. 51–58. DOI: 10.1094/CCHEM-85-1-0051.
16. Dokic, L. – Jakovljevic, J. – Dokic, P.: Relation between viscous characteristics and dextrose equivalent of maltodextrins. Starch, *56*, 2004, pp. 520–525. DOI: 10.1002/star.200400294.
17. Ahmad, F. B. – Williams, P. A. – Doublier, J.-L. – Durand, S. – Buleon, A.: Physico-chemical characterisation of sago starch. Carbohydrate Polymers, *38*, 1999, pp. 361–370. DOI: 10.1016/S0144-8617(98)00123-4.
18. Hoover, R. – Ratnayake, W. S.: Starch characteristics of black bean, chick pea, lentil, navy bean and pinto bean cultivars grown in Canada. Food Chemistry, *78*, 2002, pp. 489–498. DOI: 10.1016/S0308-8146(02)00163-2.
19. Amini, A. M. – Razavi, S. M. A. – Mortazavi, S. A.: Morphological, physicochemical, and viscoelastic properties of sonicated corn starch. Carbohydrate Polymers, *122*, 2015, pp. 282–292. DOI: 10.1016/j.carbpol.2015.01.020.
20. Singh, J. – Kaur, L. – McCarthy, O. J.: Factors influencing the physico-chemical, morphological, thermal and rheological properties of some chemically modified starches for food applications – A review. Food Hydrocolloids, *21*, 2007, pp. 1–22. DOI: 10.1016/j.foodhyd.2006.02.006.
21. Arp, C. G. – Correa, M. J. – Ferrero, C.: High-amylose resistant starch as a functional ingredient in breads: a technological and microstructural approach. Food and Bioprocess Technology, *11*, 2018, pp. 2182–2193. DOI: 10.1007/s11947-018-2168-4.
22. Miller, G. L.: Use of dinitrosalicylic acid reagent for determination of reducing sugar. Analytical Chemistry, *31*, 1959, pp. 426–428. DOI: 10.1021/ac60147a030.
23. Goñi, I. – Garcia-Alonso, A. – Saura-Calixto, F.: A starch hydrolysis procedure to estimate glycemic index. Nutrition Research, *17*, 1997, pp. 427–437. DOI: 10.1016/S0271-5317(97)00010-9.
24. Sekkal, M. – Dincq, V. – Legrand, P. – Huvenne, J. P.: Investigation of the glycosidic linkages in several oligosaccharides using FT-IR and FT Raman spectroscopies. Journal of Molecular Structure, *349*, 1995, pp. 349–352. DOI: 10.1016/0022-2860(95)08781-P.
25. Movasaghi, Z. – Rehman, S. – Rehman, I. U.: Fourier transform infrared (FTIR) spectroscopy of biological tissues. Applied Spectroscopy Reviews, *43*, 2008, pp. 134–179. DOI: 10.1080/05704920701829043.
26. Zhang, L. – Hu, X. – Xu, X. – Jin, Z. – Tian, Y.: Slowly digestible starch prepared from rice starches by temperature-cycled retrogradation. Carbohydrate Polymers, *84*, 2011, pp. 970–974. DOI: 10.1016/j.carbpol.2010.12.056.
27. Shi, Y.-C. – Seib, P. A.: Fine structure of maize starches from four *wx*-containing genotypes of the W64A inbred line in relation to gelatinization and retrogradation. Carbohydrate Polymers, *26*, 1995, pp. 141–147. DOI: 10.1016/0144-8617(94)00059-3.
28. Xie, Y.-Y. – Hu, X.-P. – Jin, Z.-Y. – Xu, X.-M. – Chen, H.-Q.: Effect of repeated retrogradation on structural characteristics and in vitro digestibility of waxy potato starch. Food Chemistry, *163*, 2014, pp. 219–225. DOI: 10.1016/j.foodchem.2014.04.102.
29. Cui, S. W.: Food carbohydrates: chemistry, physical properties, and applications. Florida: CRC Press, 2005. ISBN: 9780429095641. DOI: 10.1201/9780203485286.
30. Apostolidis, E. – Mandala, I.: Modification of resistant starch nanoparticles using high-pressure homogenization treatment. Food Hydrocolloids, *103*, 2020, article 105677. DOI: 10.1016/j.foodhyd.2020.105677.
31. Visco handbook: theory and application of viscometry with glass capillary viscometers. In: Xylem Let's Solve Water [online]. Mainz : SI Analytics, 2015 [cited 26 June 2025]. <https://www.xylemanalytics.com/en/company/blog/blog/2024/06/visco-handbook>
32. Ottenhof, M.-A. – Farhat, I. A.: Starch retrogradation. Biotechnology and Genetic Engineering Reviews, *21*, 2004, pp. 215–228. DOI: 10.1080/02648725.2004.10648056.
33. Wang, S. – Copeland, L.: Effect of acid hydrolysis on starch structure and functionality: a review. Critical Reviews in Food Science and Nutrition, *55*, 2015, pp. 1081–1097. DOI: 10.1080/10408398.2012.684551.
34. Li, W. – Cao, F. – Fan, J. – Ouyang, S. – Luo, Q. – Zheng, J. – Zhang, G.: Physically modified common buckwheat starch and their physicochemical and

structural properties. Food Hydrocolloids, *40*, 2014, pp. 237–244. DOI: 10.1016/j.foodhyd.2014.03.012.
35. Singh, N. – Kaur, L.: Morphological, thermal, rheological and retrogradation properties of potato starch fractions varying in granule size. Journal of the Science of Food and Agriculture, *84*, 2004, pp. 1241–1252. DOI: 10.1002/jsfa.1746.
36. Zeng, F. – Li, T. – Zhao, H. – Chen, H. – Yu, X. – Liu, B.: Effect of debranching and temperature-cycled crystallization on the physicochemical properties of kudzu (*Pueraria lobata*) resistant starch. International Journal of Biological Macromolecules, *129*, 2019, pp. 1148–1154. DOI: 10.1016/j.ijbiomac.2019.01.028.
37. Zhou, X. – Baik, B.-K. – Wang, R. – Lim, S.-T.: Retrogradation of waxy and normal corn starch gels by temperature cycling. Journal of Cereal Science, *51*, 2010, pp. 57–65. DOI: 10.1016/j.jcs.2009.09.005.

Received 10 April 2025; 1st revised 26 June 2025; accepted 11 August 2025.; published online 25 August 2025.